

Effect of ZnO Layers on Porous Silicon Properties

Uday Muhsin Nayef, Mohammed Waleed Muayad*, Haider Amer Khalaf

Department of Applied Science - University of Technology, Baghdad-IRAQ .

*E-mail: mwaleed1987@gmail.com

Received: 17 October 2013 / Accepted: 1 November 2013 / Published: 2 March 2014

In this paper the preparation of porous silicon (p-type) has been established by electrochemical etching and deposited by ZnO thin film using a chemical spray pyrolysis method. The results of this paper include the AFM study shows an improvement in the structural stability of the PS substrate with crystalline growth of ZnO thin film, the XRD measurement shows decreasing in crystal size of Porous Silicon after coating with ZnO, the photoluminescence spectra that explained in a blue – shifting in porous silicon layer comes from an oxidation on the porous silicon surface, and the Raman spectra shows shifting to low vibration energy level which comes from decreasing in pore diameter of the PS and decreasing in the grain size of ZnO particle.

Keywords: Porous silicon, Electrochemical etching, ZnO, AFM , Raman spectra

1. INTRODUCTION

Nanotechnology has gained substantial popularity recently due to the rapidly developing techniques both to synthesize and characterize materials and devices at the nanoscale (1-100nm). In the world of Nanotechnology, there are two grand schemes for making structures and devices such as top-down and bottom-up approaches. Top-down approaches seek to create nanoscale devices by using larger, externally-controlled ones to direct their assembly. While, bottom-up approaches seek to have smaller (usually molecular) components arrange themselves into more complex assemblies. The top-down approach often uses the traditional workshop or micro-fabrication methods where externally-controlled tools are used to cut, mill and shape materials into the desired shape and order. In contrast, bottom-up approaches use the chemical properties of single molecules to cause single-molecule components to automatically arrange themselves into some useful conformation [1]. The research in the field of Zinc Oxide/porous silicon (ZnO/PS) has attracted much attention within community as a Modern Material' because of an increasing requires for short-wavelength photonic devices, High power and High frequency electronic devices and Full cell. Where PS materials can have index large

photoluminescence (PL) Efficiency at room temperature in the visible flexibility to control and the potential applications in Si-based optoelectronic [2] and PS has since the PL Efficiency of bulk silicon is very low, due to its indirect energy band gap and short non-radiative lifetime. The reason of this was the partial dissolution of Silicon [3],

ZnO is a II-VI compound semiconductor with wide direct band-gap energy ($E_{g(ZnO)}=3.37\text{eV}$) that is suitable for short-wavelength optoelectronic applications and the high excitation binding energy (60meV) in ZnO crystal can ensure efficient excitonic emission at room temperature. ZnO is transparent to visible light and can be made high conductive by doping and its diverse growth morphologies make ZnO a key material in the field of nanotechnology and wide band-gap semiconductors [4]. When ZnO thin film deposition on Silicon substrate has received increasing interest for their lower cost and larger size. Unfortunately, the large mismatches in the lattice constant and thermal expansion coefficients would introduce a slightly large stress between the ZnO and Silicon substrate. On the other hand, the sponge-like open structure and large specific surface area make PS nanostructures a suitable material for accommodating ZnO into its pores and thus establishing a good nucleation site which is essential for the growth along the preferred orientation [5]. Due to their excellent characteristic, PS Nanostructures was used as a substrate to growth nanostructures materials such as ZnO nanostructures and Carbon nanotubes. According to Fan et. al. (1999) [6].

2. EXPERIMENTAL WORK

Experimental work consist prepared porous silicon by electrochemical anodization etching of p-type silicon <111> oriented with a resistivity 1.5-4 $\Omega\cdot\text{cm}$ and the etching cell made from Teflon because the Teflon not interaction with HF acid, rubber O-ring is used before the upper part of cell. The latter has a central circular of 1cm^2 to allow touching the silicon wafer. And the two electrodes are used to apply current across the cell. The lower one is stainless still foil below silicon wafer and the upper one is gold mesh connected with the HF solution. And after etching process, the sample were rinsed with ethanol and pentane and dried by nitrogen. After prepared PS samples,

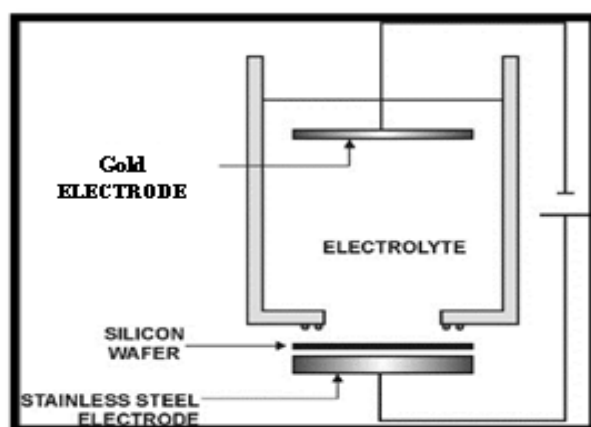


Figure 1. Electrochemical etching cell .

After that porous silicon layer coating by ZnO thin film (200nm thickness) by Thermal Spray Pyrolysis (TSP) with substrate temperature (400C^o) and spray rate (3ml/min) and deposition rate (100nm/min) and gas pressure (2Par). And study the effect of coating by (atomic force microscopy 3300AA) before and after coating , structure properties of PS ,ZnO, and ZnO/PS by XRD measurement with Cu anode tube (wavelength 0.154nm). PL Measurement and Raman Spectroscopy.

3. RESULTS AND DISCUSSION

3.1 Morphology Properties

The morphology of porous silicon with parameters (etching time: 20min, current density: 30mA/cm², and HF concentration: 15%) is showed in Fig (2).

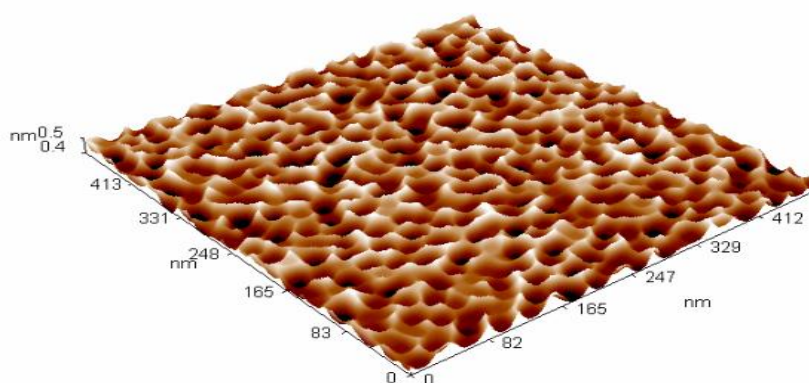


Figure 2. AFM image of porous silicon layer.

The porous silicon has higher porosity (about 85%) and lower pore diameter (18.34 nm) as indicate in Fig (2). Fig (3) shows the morphology of porous silicon after coating it by ZnO film. The film is partially filling or completely covering the pores. The surface of the PS layer is a sponge-like structure which consists of large number of ‘pores’ and voids’. These ‘pores’ and ‘voids’ make porous silicon an adhesive surface for accommodating ZnO into its pores. Thus, the ZnO thin film acted as a transparent capping and providing a good coverage of the crystallite surface on the PS substrate, which could improve the structural stability of the PS substrate [7].

Table 1. Morphology measurement data

| Sample Type | Pore Diameter(nm) | Roughness (nm) |
|-------------|-------------------|----------------|
| PS | 18.34 | 0.75 |
| ZnO/PS | 85.34 | 1.56 |

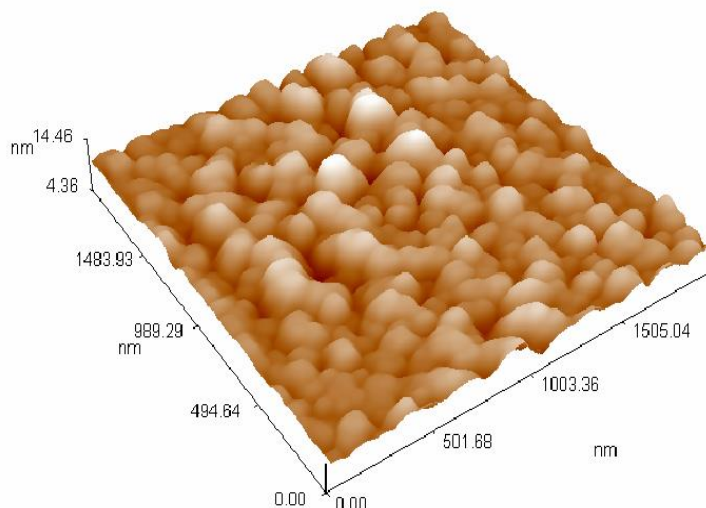


Figure 3. AFM image of ZnO thin film deposition on porous silicon layer

3.2 Structure Properties

The ZnO/PS layers exhibited a dominant diffraction peak at $2\theta = 28.3825$, corresponding to the PS (111) layer. The diffraction peak at (31.8744 ,346070,36.4616) corresponds to the (100,002,101) plane of the ZnO film, which indicates that the ZnO thin film was highly oriented along the c-axis vertical to the PS layer [8]. The broadening of the (FWHM) of the diffraction peak of the PS (111) layer was estimated from XRD. The sharp diffraction peak from the ZnO film with a weak FWHM indicates the high quality of the ZnO film [9]. The strain (ϵ_{zz}) of the nanocrystalline ZnO film grown on the PS layer along the c-axis can be calculated using the following Eq:

$$\text{Micros strain } (\epsilon\%) = \frac{c - c_0}{c_0} \tag{1}$$

where c is the lattice constant of the strained ZnO film calculated from XRD data by using eq(4.3) and (4.12) and c_0 is the unstrained lattice constant for ZnO (The lattice constants for hexagonal ZnO film are reported in JCPDS standard data $a_0=3.24982 \text{ \AA}$ and $c_0=5.20661 \text{ \AA}$).

$$\frac{1}{d^2} = \frac{4}{3} * \left(\frac{h^2 + hk + k^2}{a^2} \right) + \frac{l^2}{c^2} \tag{2}$$

Where a and c are the lattice constants of ZnO.

The obtained value of strain is -0.517%. A negative value is associated with compression strain. The low value of the compression strain revealed that the ZnO film referred to grow along the c-axis, and gave evidence of a high-quality crystal resulting.

Table 2. calculation Value of XRD measurement of PS

| Sample | 2θ (deg.) | FWHM (deg.) | d (nm) | a (nm) | L (nm) |
|----------|---------------------|----------------|-----------|-----------|-----------|
| PS <111> | 28.4152 | 2.2291 | 0.3138 | 0.5435 | 3.69 |

Table 3. calculation Value of XRD measurement of ZnO/PS

| Material | $2\theta(deg)$ | hkl | FWHM(deg) | a (nm) | c(nm) | d(nm) | L(nm) |
|----------|----------------|-----|-----------|--------|--------|-------|-------|
| PS<111> | 28.382 | 101 | 2.0559 | 0.536 | - | 0.31 | 4.00 |
| ZnO | 31.874 | 100 | 1.0667 | 0.3381 | - | 0.28 | 7.78 |
| | 34.607 | 002 | 1.0375 | - | 0.5179 | 0.25 | 8.05 |
| | 36.461 | 101 | 1.0500 | 0.3381 | 0.5179 | 0.24 | 7.99 |

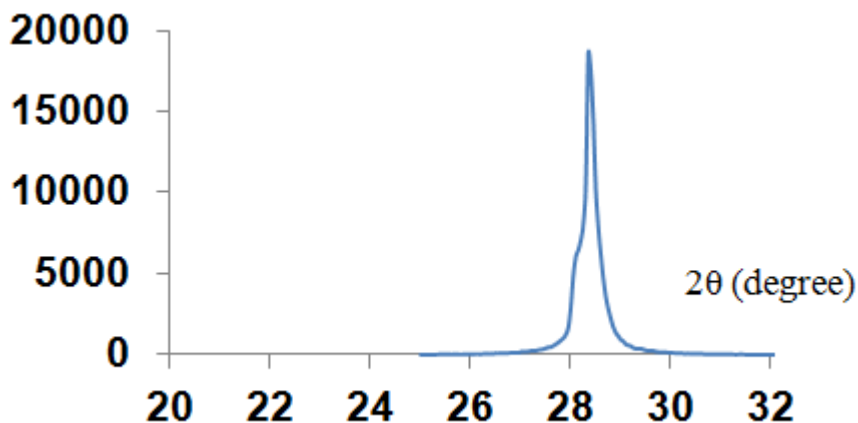


Figure 4. XRD of porous silicon <111>

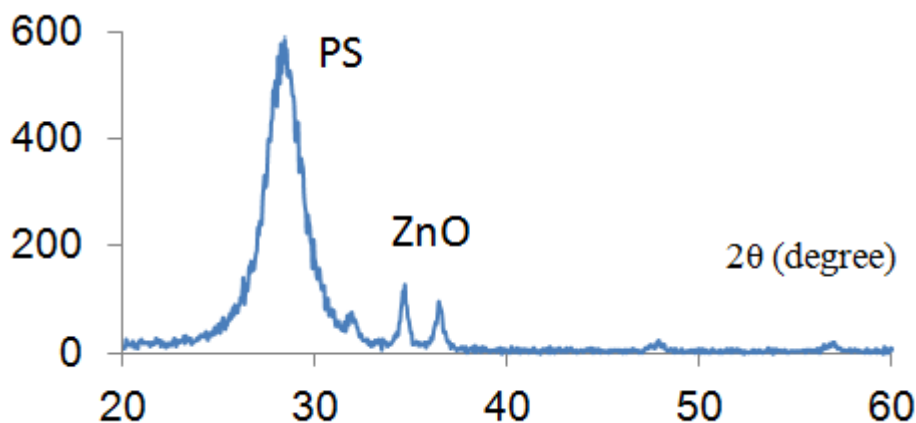


Figure 5. XRD of ZnO/PS

3.3 Photoluminescence

PL spectra of ZnO/PS layer shows that the boarding peck near 630 nm revealing the good quality of the PS, that the blue shift in PS is attributed to quantum confinement effects of electrons in nanosized particles in PS layers and the decreasing of emission wavelength of PS layers after ZnO deposition is caused by the surface oxidation which caused by ZnO thin film.

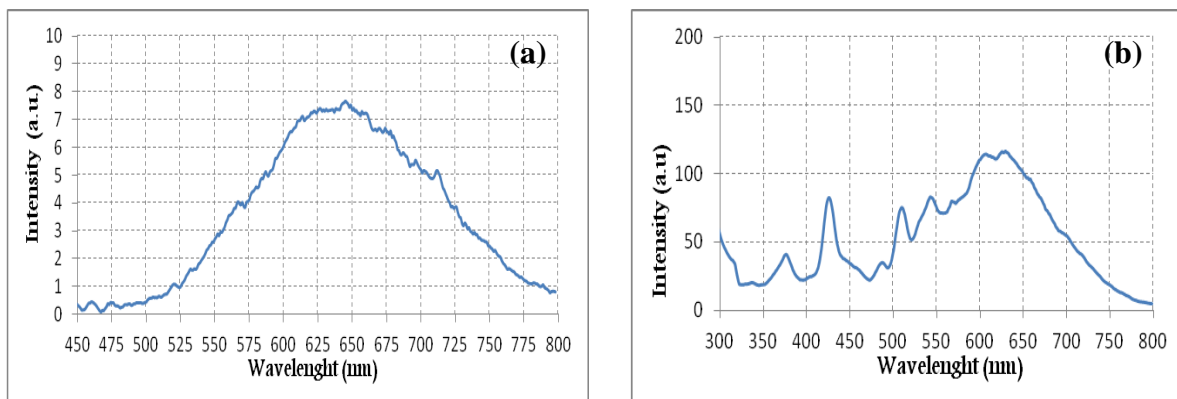


Figure 6. PL spectra of (a)PS (b)PS/ZnO

3.4 Raman Measurement

Figure (7.a) shows Raman spectral line of <111> where the broadening and the downshift of Raman peak toward lower energy indicates the presence of nanoscale features of the crystalline structures. As the size of nanocrystal decreases, the silicon optical phonon line shifts to lower frequency and becomes broader asymmetrically. The latter is more sensitive and distinct for high porosity layers of PS. The absence of other peaks in Raman spectra confirms that the prepared sample retains the crystallinity of bulk silicon wafer .

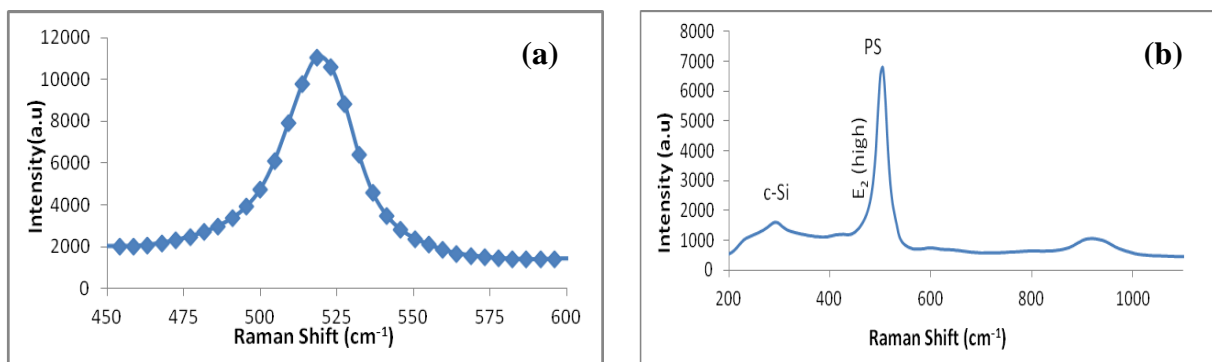


Figure 7. Raman Spectra of (a) PS (b) ZnO/PS

The optical phonon is observed in the central of Brillouin zone with energy of 520 cm^{-1} and this is due to the conservation of quasi-momentum in crystals .

Figure (7.b) shows Raman scattering spectra of ZnO/PS, the shapes of peaks at approximately 520 cm^{-1} refer to first - order scattering phonons in c-Si and this characterized the PS layers. This feature of Si nanocrystals is attributed to the quantum confinement of optical phonons in the electronic wave function of Si nanocrystals, the low frequency comes from optical phonon confinement in Si nanocrystals .

The observed phonon frequency at 305 cm^{-1} was also related to the c-Si substrate in the ZnO/PS layers. The ZnO wurtzite hexagonal crystal structure belongs to space group C_{6m}^4 in the group theory with two formulae units per primitive cell. Therefore, the Raman-active zone center for optical phonons is $2A_1 + 2B_1 + 2E_1 + 2E_2$, where A_1 and E_1 symmetry are polar phonon modes with two different frequencies for transverse - optical (TO) and longitudinal - optical (LO) phonons, respectively. The $2B_1$ are silent modes. The E_2 symmetry is a nonpolar phonon mode with two

frequencies: E_2 (high), is related to oxygen atoms, and E_2 (low), is related to the zinc sub-lattice. The E_2 (high) mode shows a band at 492 cm^{-1} related to E_2 (high) due to oxygen atoms present after the ZnO deposition.

4. CONCLUSION

From the results we conclude that the surface stability of PS is increased after deposition ZnO film on it as increasing in the spectra boarding in XRD spectra which is noticed in the shifting, and the frequency of the optical and acoustic mode for both PS and ZnO are decreasing due to conferment particle in nanodimension .

References

1. M. Kohler, W. Fritzsche, "Nanotechnology: an Introduction to Nanostructuring Technique", WILEY-VCH , (2004).
2. R. Smith, S. Collins, *Journal of Applied. Physic*, 71 (1992)R1–R22
3. O. Bisi , S. Ossicini , L. Pavesi, *Surface Science Reports*, 38 (2000) 1-126
4. M. Basak. *Materials Research Bulletin*, 42(2007) 875-882
5. R.G. Singh, Fouran Singh, V. Agarwal , R.M. Mehra, *Journal of Physics D*, 40(2007) 3090-3093
6. S.S. Fan, M.G. Chapline, N.R. Franklin, T.W. Tomblor, A.M. Cassell, H.J. Dai, *Science Journal*, 283(1999) 512.
7. S.M. Thahab, *Optoelectronics and Advanced Materials*, 11 (2011)1107-1110
8. N. Izni , M. Tankikawa , M. R. Mahmood, K. Yasui, A.M. Hashim, *Materials Journal*, 5 (2012) 2817-2832.
9. K. A. Salman, K. Omar, Z. Hassan, *Solar Energy Journal*, 86 (2011) 541-546

© 2014 The Authors. Published by ESG (www.electrochemsci.org). This article is an open access article distributed under the terms and conditions of the Creative Commons Attribution license (<http://creativecommons.org/licenses/by/4.0/>).